ADVANCED MATERIALS
www.advmat.de

Spider-Silk-Inspired Nanocomposite Polymers for Durable Daytime Radiative Cooling

Pengcheng Yao, Zipeng Chen, Tianji Liu, Xiangbiao Liao, Zhengwei Yang, Jinlei Li, Yi Jiang, Ning Xu, Wei Li, Bin Zhu, and Jia Zhu**

Passive daytime radiative cooling (PDRC) materials, that strongly reflect sunlight and emit thermal radiation to outer space, demonstrate great potential in energy-saving for sustainable development. Particularly, polymer-based PDRC materials, with advantages of easy-processing, low cost, and outstanding cooling performance, have attracted intense attention. However, just like other polymer devices (for example polymer solar cells) working under sunlight, the issue of durability related to mechanical and UV properties needs to be addressed for large-scale practical applications. Here, a spider-silk-inspired design of nanocomposite polymers with potassium titanate ($K_2Ti_6O_{13}$) nanofiber dopants is proposed for enhancing the durability without compromising their cooling performance. The formed tough interface of nanofiber/polymer effectively disperses stress, enhancing the mechanical properties of the polymer matrix; while the $K_2Ti_6O_{13}$ can absorb high-energy UV photons and transform them into less harmful heat, thereby improving the UV stabilities. Taking poly(ethylene oxide) radiative cooler as an example for demonstration, its Young's modulus and UV resistance increase by 7 and 12 times, respectively. Consequently, the solar reflectance of nanocomposite poly(ethylene oxide) is maintained as constant in a continuous aging test for 720 h under outdoor sunlight. The work provides a general strategy to simultaneously enhance both the mechanical stability and the UV durability of polymer-based PDRC materials toward large-scale applications.

1. Introduction

While traditional cooling technologies based on electricity consume tremendous amounts of energy and produce huge carbon emissions,[1–3] passive daytime radiative cooling (PDRC) is emerging as an appealing cooling strategy,[4–8] which reflects most of the sunlight (0.3–2.5 µm) and radiates heat to outer space through the atmospheric transparency window (8–13 µm).[9,10] Among various materials demonstrated to realize PDRC, polymer-based PDRC materials show great potential because of the intrinsic high emissivity in mid-infrared and easy-processing features for large-scale applications.[11–13]

However, just like other polymer devices (such as polymer solar cells) working under outdoor conditions, the stability issues of polymer-based PDRC materials, particularly mechanical stabilities and photostabilities (ultraviolet irradiation), need to be further addressed. Specifically, polymer-based PDRC materials are prone to mechanical failure because of environmental stresses when working outdoors. What is worse, the long-term UV irradiation from sunlight will further accelerate the weakening of the mechanical properties and cause yellowish color for most polymers (declined reflectance), making the PDRC ineffective.[14]

Compared to other polymer devices, the issues of the mechanical stabilities for PDRC polymers are more challenging, as their mechanical properties are compromised by the porosity requirement for daytime radiative cooling. The key for polymer materials to realize net daytime radiative cooling is to increase the R_{Solar},[15] as polymers typically possess desirable high ε_{LWIR} due to their natural molecular bond vibrations in the mid-infrared region. Considering the sunlight irradiance of 1000 W m^{-2} in the daytime, even a small amount of solar energy absorption of PDRC materials would offset the effect of radiative cooling (**Figure 1**a,b). Therefore, achieving net cooling power dictates that at least over 90% of sunlight must be reflected ($R_{Solar} \approx 0.9$) (detailed in Supporting Information).

As a result, porous structures with air holes at wavelength scale have been employed (via techniques such as electrospinning and solvent evaporation) to create strong multiple

P. Yao, Z. Chen, Z. Yang, J. Li, Y. Jiang, N. Xu, B. Zhu, J. Zhu
National Laboratory of Solid State Microstructures
College of Engineering and Applied Sciences
Jiangsu Key Laboratory of Artificial Functional Materials
Collaborative Innovation Center of Advanced Microstructures
Nanjing University
Nanjing 210023, P. R. China
E-mail: binzhu@nju.edu.cn; jiazhu@nju.edu.cn
T. Liu, W. Li
GPL Photonics Laboratory
State Key Laboratory of Applied Optics
Changchun Institute of Optics
Fine Mechanics and Physics
Chinese Academy of Sciences
Changchun 130033, P. R. China
X. Liao
Advanced Research Institute of Multidisciplinary Science
Beijing Institute of Technology
Beijing 100081, P. R. China
The ORCID identification number(s) for the author(s) of this article can be found under https://doi.org/10.1002/adma.202208236.

DOI: 10.1002/adma.202208236

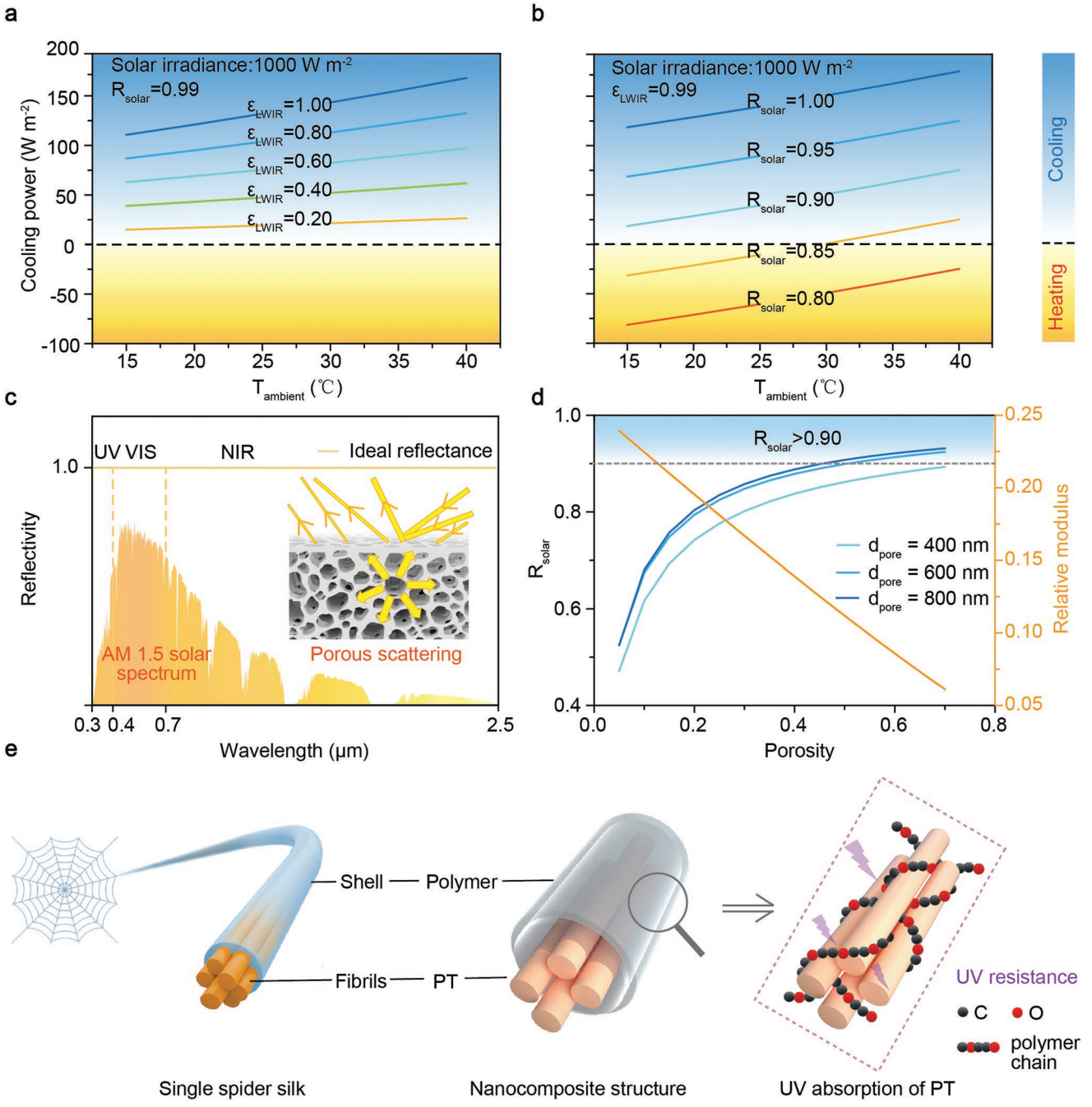

Figure 1. a) Cooling power versus ambient temperature ($T_{ambient}$) when ε_{LWIR} changes from 0.2 to 1 (R_{solar} = 99%). b) Cooling power versus ambient temperature when R_{solar} changes from 0.8 to 1.0 (ε_{LWIR} = 99%). c) Ideal reflectance curve in the solar band and the scattering of porous structures in polymer-based PDRC materials. d) The relationship between relative modulus and R_{Solar} as a function of porosity, which shows the trade-off between the reflectivity and mechanical properties given a porosity range. e) Spider-silk-inspired nanocomposite designs with enhanced mechanical properties. $K_2Ti_6O_{13}$ absorbs high-energy UV photons.

scattering at air holes/polymer interfaces,[16,17] thus enhancing sunlight reflection (Figure 1c).[18] However, according to mechanical theory, there exists a trade-off between the porosity and mechanical stability (measured by Young's modulus) of polymer-based PDRC.[19,20] As illustrated clearly in Figure 1d (Figures S1 and S2, Supporting Information for analysis), the high reflectivity rising from porous structures sacrifices PDRC materials' stiffness compared to their solid phase. Therefore, simultaneously achieving high reflectivity and excellent mechanical properties in PDRC polymers pose a significant challenge.

It is well-known that spider silk, possesses outstanding mechanical properties owing to its hierarchically ordered structures (Figure 1e), thus easily constituting a mechanically strong

web with porosities for predation.[21–23] Herein, inspired by spider silk, we demonstrated polymer-based PDRC materials with significantly enhanced mechanical and photostabilities, through potassium titanate ($K_2Ti_6O_{13}$) nanofibers doped nanocomposite structure (Figure 1e).[24,25] To effectively enhance the mechanical properties and UV stabilities without affecting the optical properties of PDRC polymers, the option of dopant is critical. There are unique advantages of doping $K_2Ti_6O_{13}$ (PT) nanofibers in PDRC polymers. First, PT itself has a high R_{Solar} of 95.4% and ε_{LWIR} of 94.8% (Figures S3 and S4, Supporting Information), which is not detrimental to the optical properties of PDRC polymers. Second, PT features a high tensile strength of 7 GPa and a tensile modulus of 280 GPa, stronger than glass fibers and even comparable to carbon fibers.[26–28] Third, $K_2Ti_6O_{13}$ can absorb high-energy UV photons and transform them into less harmful heat, preventing the polymer from being damaged (Figure 1e and details see below).

As a demonstration with poly(ethylene oxide) (PEO) porous film as the radiative cooler, we observed the enhancement of the strength, elongation at break, Young's modulus, and UV stability of nanocomposite PEO film by 2.3, 1.6, 7, and 12 times, respectively, with its optical properties retained. Consequently, we achieved a high-performing and stable cooling power of 92 W m^{-2} for over continuous 720 h under sunlight. Our work offers a general strategy to improve both the mechanical and UV stability of PDRC polymers with high radiative cooling performance, and therefore paving the way for their large-scale production and practical applications.

2. Results

Porous PEO film has shown a good radiative cooling performance but limited durability.[14] Here we processed the PEO with the PT nanofibers dopant to examine the feasibility of the nanocomposite design illustrated above. First, we synthesized PT@PEO films through a scalable roll-to-roll electrospinning method reported in our previous work (Figure S5, Supporting Information).[15] **Figure 2**a demonstrates a PT@PEO (mass ratio of 1:10) film with a length of several meters. The white color indicates its strong scattering of visible light, which is ascribed to the connection of fibers and the formed numerous multiple pores (Figure 2b; Figures S6–S8, Supporting Information). Specifically, a high reflectivity of ≈0.94 is achieved in the solar wavelength, and the emissivity in 8–13 μm reaches 0.91 (Figure 2c; Figure S9, Supporting Information), ideal for radiative cooling.

To verify the construction of hierarchical structure in PT@PEO films, transmission electron microscopy (TEM) tests of the single fiber were conducted. The results match well with spider silk structures (Figure 2d; Figure S10, Supporting Information). The partially enlarged view (Figure 2e) and EDS mapping (Figure 2f) of PT@PEO fiber show that the introduced PT nanowires are wrapped inside the PEO polymer and form a hierarchical and nanocomposite structure. In addition, analysis by X-ray Diffraction (XRD) and Fourier transform infrared (FTIR) verify that the components of both PEO polymer and PT nanowires remain unchanged (Figure 2g,h).

In order to demonstrate the tensile behavior of the obtained hierarchical structure, finite element simulations were carried out with a typical nanocomposite fiber (PT nanofibers axially oriented inside a PEO matrix). The stress in the PEO phase is much lower than that of PT nanofiber fillers subjected to axial tension (Figure 2i, detailed in Supporting Information). It is due to that while the volume fraction of nanofibers is small, the stiff nanofibers mainly bear the external force, and the tough interface of nanofiber/polymer transfers the stress to the polymer matrix. The simulation shows that the Young's modulus of PT@PEO nanocomposite fiber is enhanced by 700% compared to that of pure PEO (Figure 2j).

The enhancement in mechanical properties is further demonstrated as the stress–strain responses of pure PEO electrospinning film and PT@PEO film at a constant tensile strain rate of 0.01 m min^{-1}. Various mass ratios of PT@PEO were also investigated (Figure S11, Supporting Information), it is found that at the mass ratio of 1:10, PT@PEO films exhibit the best mechanical performance. Adding 10 wt.% PT nanowires to the PEO PDRC film significantly improves Young's modulus from 27.88 to 190.82 MPa of the membrane (**Figure 3**a). Also, the tensile stress and the elongation at break are increased by 230% and 160%, respectively. The above optimizations realize an all-around enhancement of mechanical properties compared with initial PEO films (Figure 3a). As for UV stability, after 1.5 h UV aging accelerated test at 10 cm away from 500 W mercury lamp, PT@PEO films still maintained their initial tensile strength and elongation at break, while pure PEO films showed a sharp decline with the extension of irradiation time (Figure 3b,c). In order to intuitively demonstrate the difference in their UV resistance, we conducted a long-time (12 h) UV radiation process. It was obvious that pure PEO films were completely broken and presented pulverization once encountering a little external force. By comparison, PT@PEO films can still withstand considerable stretching or twisting forces, exhibiting outstanding UV durability (Figure 3d; Movies S1–S4, Supporting Information).

To unveil the underlying mechanism of UV stability enhancement, we first characterized the microstructures of pure PEO and PT@PEO nanocomposites after different UV exposure times. As shown in Figure 3e, UV radiation makes it difficult for pure PEO fibers to maintain multilayer network structures, and the fibers are gradually broken. On the contrary, PT@PEO fibers still keep their stable porous network structures, ensuring the overall mechanical performance (Figure 3f). What's more, FTIR tests were carried out to explore the chemical changes in PDRC PEO and PT@PEO nanocomposite. The massive energy in UV bands will break the C—O—C bond in PEO and form carbonyl (C=O) (Figure 3g). This process leads to the oxidation of PEO and thus resulting in poor UV durability. In particular, oxidation and carbonyl formation processes are one of the main reasons for the UV aging of most polymers.[29] Surprisingly, the addition of PT greatly restrains the formation of carbonyl. There is no obvious C=O signal even after 12 h UV radiation in PT@PEO films (Figure 3h), which indicates the significantly enhanced UV stability. All of these experimental results verify that the addition of PT can greatly improve the UV stability of PEO.

To further understand the underlying mechanism, we first measured the UV–vis spectra of PEO, PT, and PT@PEO

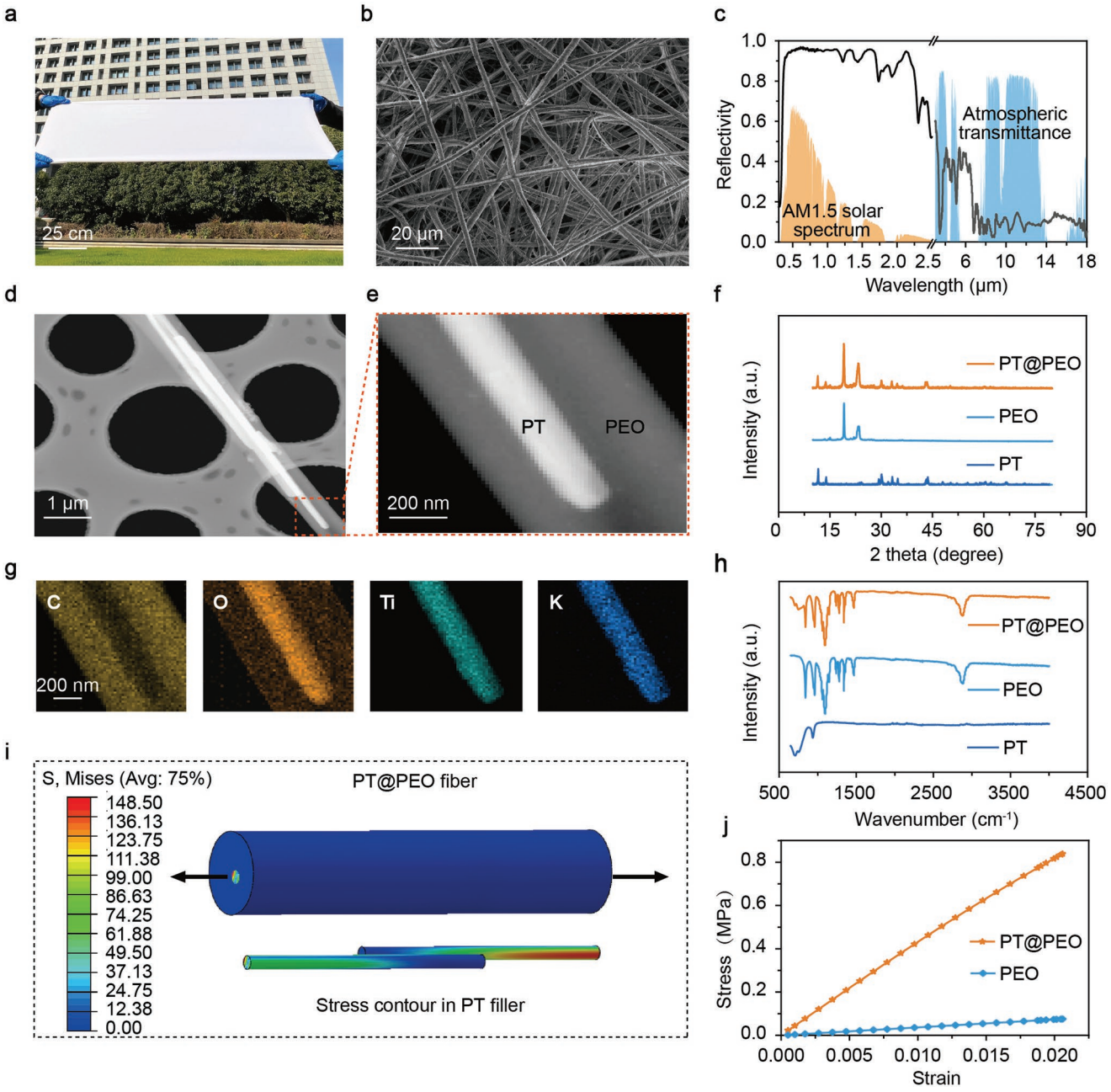

Figure 2. a) Photograph of PT@PEO films. b) SEM images of random nanofibres of PT@PEO films. c) Reflectivity spectrum of PT@PEO film in 0.3–18 μm wavelength range presented against the AM1.5 solar spectra and the atmospheric transparency windows. d,e) TEM images (d) with their partial enlarged view (e) and f) EDS mapping of C, O, Ti, K elements of PT@PEO nanocomposite fiber. g) XRD patterns and h) FTIR spectra of PT powder, PEO film, and PT@PEO film. i) The contour of von Mises stress in a fiber structure with PT nanofibers axially oriented inside a PEO polymer matrix under axial tension, the diameters of PT@PEO fiber and PT nanofibers are 1.5 μm and 250 nm, respectively. j) Stress–strain curve of the PT@PEO nanocomposite fiber under axial tension, and the modulus of nanocomposite and pure PEO is calculated to be 40.57 and 3.67 MPa, respectively.

(Figure S12, Supporting Information). It is clearly seen in Figure S12 (Supporting Information) that PT has good absorption in the UV range, thus most of the carriers generated after absorption can be recombined in the bulk or the surface, and converted into other harmless forms such as heat (Figure 3i). The photocurrent tests show that PT has lower photocurrent density compared with traditional UV screening agents (rutile TiO_2). It suggests that the photo-generated electrons are prone to recombine in PT to convert UV radiation into heat (Figure S13, Supporting Information), consequently resulting in the better UV durability of PT@PEO samples.

As a result, adding PT nanowires into PDRC polymers to form the nanocomposite structures will improve their potential as a mechanically robust and durable material for PDRC applications, while the optical properties for radiative cooling are retained (Figure 3j).

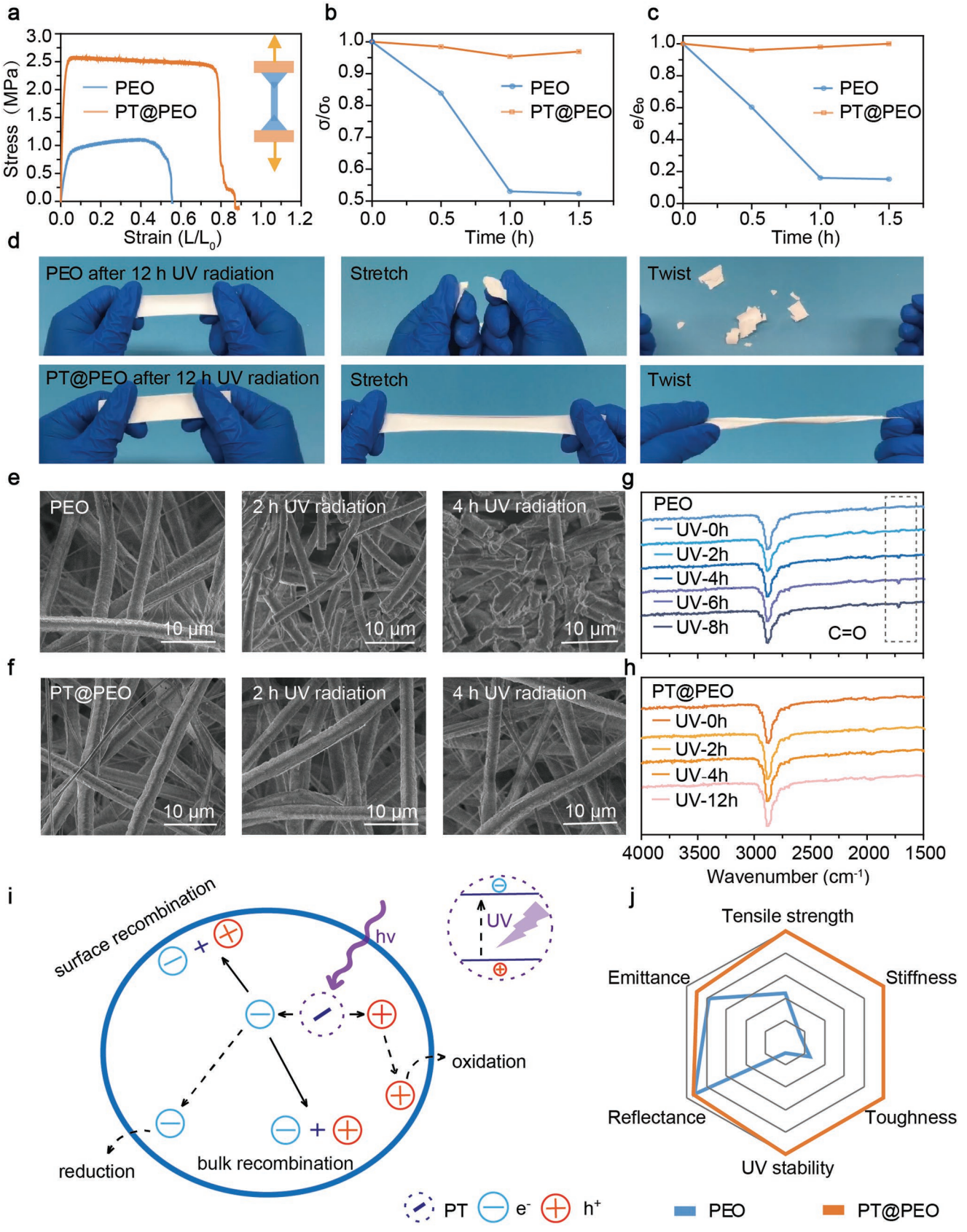

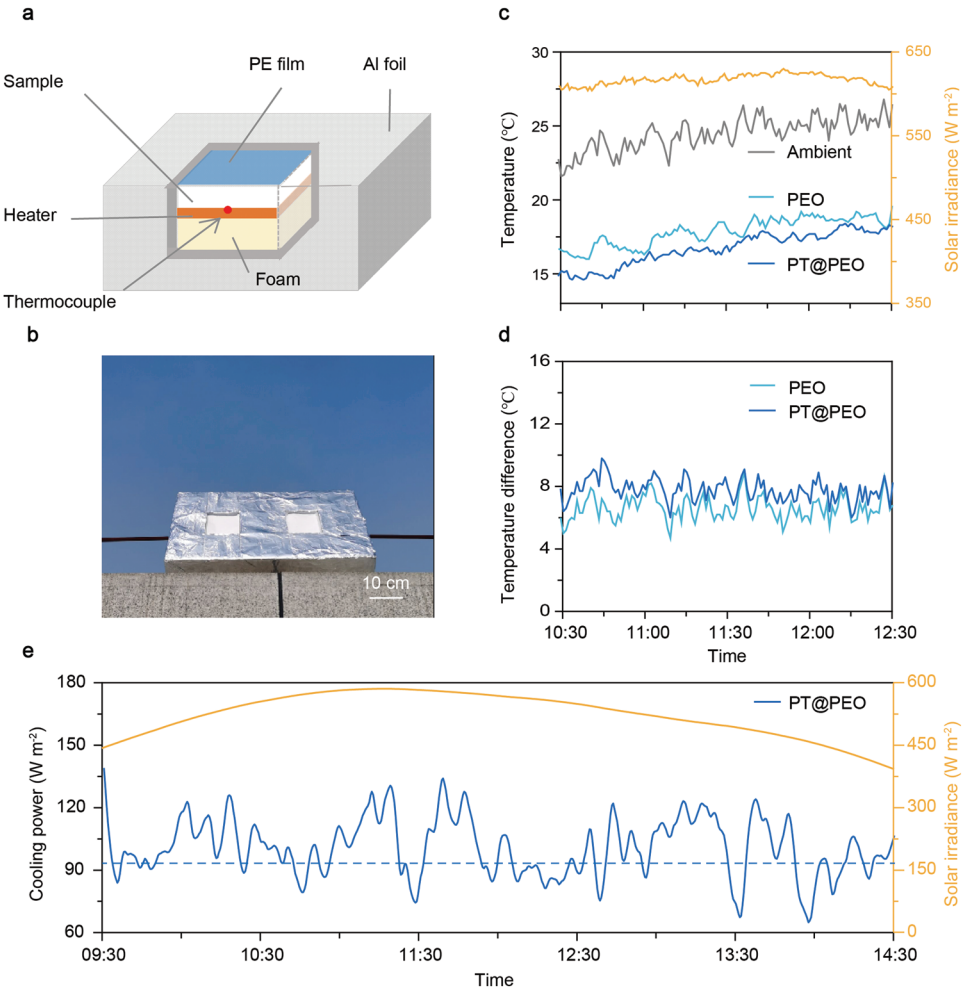

Figure 4. a) Schematic of the radiative cooling set-up for testing performance. b) Set-up of the real-time measurement of the radiative cooling performance. c) Temperature measured for ambient air, and PT@PEO and pure PEO films and d) their temperature difference of the outdoor experiment in Nanjing (date: 15 November 2021). e) Cooling power of the PT@PEO film, along with the solar irradiance (date: 6 December 2021).

To experimentally confirm the nanocomposite polymer preserving its excellent radiative cooling performance, we performed continuous outdoor measurements on both PT@PEO and pure PEO films on a clear day in Nanjing (Figure S14, Supporting Information). As shown in **Figure 4**a,b, two samples were placed side by side in similar experimental devices. All the tests were conducted simultaneously under the same conditions, especially the air temperature and solar irradiance. In the daytime (from 10:30 a.m. to 12:30 p.m.) under sunlight, the temperatures of both films were consistently below the ambient temperature (Figure 4c), while the PT@PEO film realized a sub-ambient temperature drop of ≈8 °C (Figure 4d). Even under the solar irradiance of about 600 W m^{-2} at noon, the corresponding cooling power of the PT@PEO film reached as high as 92 W m^{-2} (Figure 4e). The results illustrate that the introduction of PT nanowires in PEO fibers still retains the excellent radiative cooling performance of the PDRC polymers.

To demonstrate the stability of the obtained PT@PEO under outdoor conditions, 100 cm^2 square films of PEO PDRC polymers and PT@PEO nanocomposite polymers were put outdoors for a continuous 30-day stability test. The results show as the outdoor exposure time increases, pure PEO PRDC films began to have cracks on the surface and gradually broke into pieces. In contrast, PT@PEO films remained intact after 30 days of outdoor placement (**Figure 5**a, Supporting Information for details). In addition, the reflectance of pure PEO films decreased below 90% after 15 days because of the UV yellowing, almost losing their sub-ambient cooling performance (Figure 1b). On the contrary, PT@PEO films remained at their origin high R_{solar} with the increase of days (Figure 5b). The results further illustrate the

Figure 3. a) Stress–strain curves of the PEO and PT@PEO film, and the PT@PEO film shows greater strength and toughness (elongation at break). b) With the increase of UV irradiation time, the variation trend of the tensile strength and c) elongation at break relative to the initial value of the films. d) Optical pictures of PEO and PT@PEO films after UV irradiation. e,f) SEM images of PEO and PT@PEO films after UV irradiation. g,h) FTIR spectra of PEO (g) and PT@PEO (h) film films after different UV irradiation times. i) Underlying mechanism of PT for enhanced UV stability. j) Radar plots comparing the performance of pure PEO and PT@PEO films.

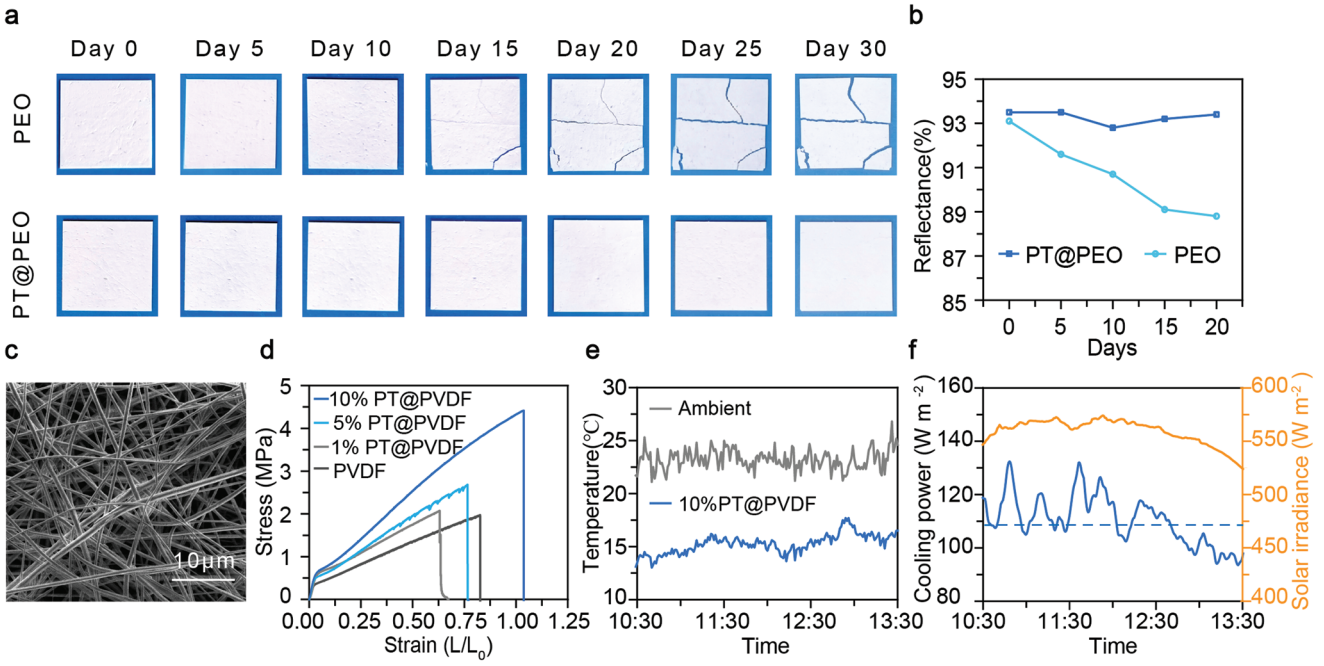

Figure 5. a) Outdoor physical maps of PT@PEO and pure PEO films (size: 100 cm^2) for 30 days. b) Relationship between reflectivity and days. c) Scanning electron microscopy (SEM) images of PT@PVDF films. d) Stress–strain curves of PT@PVDF film under different PT additions. e) The temperature data and f) cooling power measured for PT@PVDF films.

outstanding stabilities of PT@PEO films owing to the introduction of PT nanowire fillers into PEO fibers.

As processing with PT nanofibers dopant is a generalized design, it can be applied to various other polymer systems, such as polyvinylidene fluoride (PVDF) (another PDRC polymer reported before). The SEM image of PT@PVDF nanocomposite films prepared by electrospinning shows the connection of nanofibers and multiple pores (Figure 5c), ensuring high R_{Solar}. By adjusting the addition amount of PT, we found that the modification effect was optimum when the addition amount and polymer matrix reached a 1:10 mass ratio (Figure 5d), which significantly improved both the strength and toughness of PVDF films. Furthermore, such nanocomposite film maintains a high reflectivity (96.5%) in the solar band and high emissivity (95.1%) in the atmospheric windows (Figure S15, Supporting Information), promising for excellent radiative cooling performance (Figure 5e,f).

3. Conclusions

We have demonstrated a spider-silk-inspired nanocomposite strategy for building polymer-based PDRC materials with enhanced mechanical properties and UV durability. As a demonstration with PEO PDRC, by introducing potassium titanate nanofibers, its Young's modulus and UV resistance were increased by 7 and 12 times, respectively. As a result, the cooling performance of PT@PEO does not show any decline for over 720 h under natural sunshine. Additionally, such a nanocomposite method presents a universal reinforcing effect in various matrix materials. Therefore, our work provides a new pathway to fundamentally improve both the mechanical and the UV stability of polymer-based PDRC materials toward practical applications.

Supporting Information

Supporting Information is available from the Wiley Online Library or from the author.

Acknowledgements

P.C.Y. and Z.P.C. contributed equally to this work. The authors acknowledge the micro-fabrication center at the National Laboratory of Solid State Microstructures (NLSSM) for technical support. This work was jointly supported by the National Key Research and Development Programme of China (numbers 2021YFA1400700 and 2020YFA0406104), National Natural Science Foundation of China (numbers 52002168, 12022403, 11874211, and 61735008), Science Foundation of Jiangsu (BK20190311), Key Science and Technology Innovation Programme of Shandong Province (2019JZZY020704), Excellent Research Programme of Nanjing University (ZYJH005), and the Fundamental Research Funds for the Central Universities (numbers 021314380184, 021314380190, and 021314380214). J.Z. acknowledges support from the XPLORER PRIZE.

Conflict of Interest

The authors declare no conflict of interest.

Data Availability Statement

The data that support the findings of this study are available from the corresponding author upon reasonable request.

Keywords

durability, passive daytime radiative cooling, poly(ethylene oxide), potassium titanate, radiative cooling

Received: September 7, 2022
Revised: October 11, 2022
Published online:

[1] B I. Cook, J E. Smerdon, R. Seager, S. Coats, *Clim. Dyn.* **2014**, *43*, 2607.
[2] S. Vall, A. Castell, *Renewable Sustainable Energy Rev.* **2017**, *77*, 803.
[3] A. Baniassadi, D J. Sailor, G A. Ban-Weiss, *Urban Clim.* **2019**, *29*, 100495.
[4] B. Zhu, W. Li, Q. Zhang, D. Li, X. Liu, Y. Wang, N. Xu, Z. Wu, J. Li, X. Li, P B. Catrysse, W. Xu, S. Fan, J. Zhu, *Nat. Nanotechnol.* **2021**, *16*, 1342.
[5] Po-C Hsu, A Y. Song, P B. Catrysse, C. Liu, Y. Peng, J. Xie, S. Fan, Yi Cui, *Science* **2016**, *353*, 1019.
[6] S. Zeng, S. Pian, M. Su, Z. Wang, M. Wu, X. Liu, M. Chen, Y. Xiang, J. Wu, M. Zhang, Q. Cen, Y. Tang, X. Zhou, Z. Huang, R. Wang, A. Tunuhe, X. Sun, Z. Xia, M. Tian, M. Chen, X. Ma, L. Yang, J. Zhou, H. Zhou, Q. Yang, X. Li, Y. Ma, G. Tao, *Science* **2021**, *373*, 692.
[7] S. Fan, W. Li, *Nat. Photonics* **2022**, *16*, 182.
[8] T. Li, Y. Zhai, S. He, W. Gan, Z. Wei, M. Heidarinejad, D. Dalgo, R. Mi, X. Zhao, J. Song, J. Dai, C. Chen, A. Aili, A. Vellore, A. Martini, R. Yang, J. Srebric, X. Yin, L. Hu, *Science* **2019**, *364*, 760.
[9] W. Li, S. Fan, *Opt. Photonics News* **2019**, *30*, 32.
[10] D. Zhao, A. Aili, Y. Zhai, S. Xu, G. Tan, X. Yin, R. Yang, *Appl. Phys. Rev.* **2019**, *6*, 021306.
[11] A. Aili, Z. Y. Wei, Y. Z. Chen, D. L. Zhao, R. G. Yang, X. B. Yin, *Mater Today Phys* **2019**, *10*, 100127.
[12] T. Wang, Yi Wu, L. Shi, X. Hu, M. Chen, L. Wu, *Nat. Commun.* **2021**, *12*, 365.
[13] Y. Zhai, Y. Ma, S N. David, D. Zhao, R. Lou, G. Tan, R. Yang, X. Yin, *Science* **2017**, *355*, 1062.
[14] S. H. Hamid, *Handbook of Polymer Degradation*, CRC Press, Boca Raton, FL, USA **2000**.
[15] D. Li, X. Liu, W. Li, Z. Lin, B. Zhu, Z. Li, J. Li, Bo Li, S. Fan, J. Xie, J. Zhu, *Nat. Nanotechnol.* **2021**, *16*, 153.
[16] J. Li, Y. Liang, W. Li, N. Xu, B. Zhu, Z. Wu, X. Wang, S. Fan, M. Wang, J. Zhu, *Sci. Adv.* **2022**, *8*, eabj9756.
[17] J. Mandal, Y. Fu, A C. Overvig, M. Jia, K. Sun, N N. Shi, H. Zhou, X. Xiao, N. Yu, Y. Yang, *Science* **2018**, *362*, 315.
[18] M. Chen, D. Pang, J. Mandal, X. Chen, H. Yan, Y. He, N. Yu, Y. Yang, *Nano Lett.* **2021**, *21*, 1412.
[19] G. Qian, X. Liao, Y. Zhu, F. Pan, Xi Chen, Y. Yang, *ACS Energy Lett.* **2019**, *4*, 690.
[20] Y. Yang, Y. Zhang, *MRS Energy Sustainability* **2020**, *7*, E18.
[21] A P. Kiseleva, P V. Krivoshapkin, E F. Krivoshapkina, *Front. Chem.* **2020**, *8*, 554.
[22] Y. Dou, Z. -. P. Wang, W. He, T. Jia, Z. Liu, P. Sun, K. Wen, E. Gao, X. Zhou, X. Hu, J. Li, S. Fang, D. Qian, Z. Liu, *Nat. Commun.* **2019**, *10*, 5293.
[23] K. Bourzac, *Nature* **2015**, *519*, S4.
[24] J. Cid-Dresdnerhildabuergerm, *Z. Kristallogr.* **1962**, *117*, 411.
[25] K. K. Somashekharappa, S. V. Lokesh, *ACS Omega* **2021**, *6*, 7248.
[26] R. Luo, Y. Ni, J. Li, C. Yang, S. Wang, *Mater. Sci. Eng. A* **2011**, *528*, 2023.
[27] B A. Newcomb, *Composites, Part A* **2016**, 262.
[28] J. Wang, Y. Zhang, L. Tian, H. Wang, T. Wang, C. Feng, J. Xia, S. Zhang, *Optik* **2020**, *223*, 165547.
[29] R. Seldén, B. Nyström, R. Långström, *Polym. Compos.* **2004**, *25*, 543.